Fizika Nizkikh Temperatur, 2007, v. 33, Nos. 2/3, p. 153–164

Tunneling and magnetic properties of triple quantum dots

K. Kikoin

Raymond and Beverly Sackler Faculty of Exact Sciences, School of Physics and Astronomy
Tel-Aviv University, Tel-Aviv 69978, Israel
E-mail: kikoin@bgu.ac.il

Received November 7, 2006

Unconventional features of Kondo effect in quantum tunneling through triple quantum dots are reviewed. Special attention is paid to the interplay between continuous rotation symmetries in the spin space and discrete point symmetries in the real space. Specific properties of Kondo effect in linear, cross, fork and triangular configurations of triple quantum geometries dot are discussed.

PACS: 72.10.Fk Scattering by point defects, dislocations, surfaces, and other imperfections (including Kondo effect);
73.21.La Quantum dots.

Keywords: Kondo effect, quantum tunneling, triple quantum geometries.

Introduction

Soon after Kondo's breakthrough in explanation for the puzzling shallow minimum in the temperature dependent resistivity of metals doped by magnetic impurities [1], theoreticians started to extend this promising conceptual framework for other physical situations and for more complex objects than simple localized moments. His original idea was formulated within the framework of a well established Hamiltonian describing exchange between the impurity spin $\mathbf{S_j}$ located on a given site j and the spin pertaining to a Fermi sea of conduction electrons. The latter is represented by itinerant spin $\mathbf{s_{kk'}} = c^{\dagger}_{\mathbf{k}\sigma}\hat{\tau}c_{\mathbf{k}'\sigma'}$ projected on the impurity site $\mathbf{j}$, namely $\mathbf{s_j} = \sum_{\mathbf{kk}'} \mathbf{s_{kk'}} \exp i(\mathbf{k}-\mathbf{k}')\cdot\mathbf{j}$. Here $\hat{\tau}$ is the vector of Pauli matrices for a spin $1/2$. The so called *sd*-exchange Hamiltonian is,

$$H_{sd} = \sum_{\mathbf{k},\sigma} \varepsilon_k c^{\dagger}_{\mathbf{k}\sigma} c_{\mathbf{k}\sigma} + J\mathbf{S_j}\cdot\mathbf{s_j}, \qquad (1)$$

where ε_k is the energy dispersion of the itinerant electrons and J is the exchange coupling constant. The internal degrees of freedom involved in Kondo effect are classified in terms of $SU(2)$ group of continuous rotations in the spin sector of Fock space.

It was recognized that the Kondo mechanism should work also in systems exhibiting electron tunneling, where two metallic slabs are separated by thin dielectric layer, which forms a tunnel barrier for electrons in the slabs. It was shown [2,3] that the magnetic impurity located somewhere near the tunneling layer plays the same role in tunnel conductance as magnetic impurity immersed in a metal (and has exchange interaction with Fermi sea electrons) does for impurity resistance. It was also shown [4] that the Friedel–Anderson model [5,6] for resonance scattering of conduction electrons by the electrons occupying the 3*d*-levels of transition metal impurities can be mapped on the exchange Hamiltonian (1) provided the strong Coulomb interaction in the 3D shell suppresses charge fluctuations on the impurity site. In the next stage of development, orbital degrees of freedom were incorporated in the Kondo physics. The basic idea of this generalization was that the magnetic impurity being put in the center of the coordinates imposes its point symmetry on otherwise translationally invariant crystal, and the adequate description of scattered waves should be based on the partial wave expansion (either in spherical waves [5] or in cubic harmonics [7]). Based on this idea, the generalized Schrieffer–Wolff model was proposed [8,9], where the magnetic impurity is described as an effective N-component moment, but the exchange scattering is not restricted by the usual spin selection rule $\Delta m = 0, \pm 1$ for the projection m of this moment. Another version of this model allots the impurity and band states both by spin and orbital (referred to as «color» in the general case) index. In case of spin $s = 1/2$ and N colors the symmetry of the impurity is

$SU(2N)$ [10,11]. Appearance of additional degrees of freedom in the Kondo Hamiltonian might lead to the interesting scenario of overscreened Kondo effect, which arises when the number of conduction electron «colors» exceed that of impurity moment [12]. This effect is characterized by the non-Fermi-liquid low-temperature thermodynamics unlike the standard Kondo effect, which only modifies (although radically) the Fermi liquid properties of undoped metal [13].

A powerful incentive for further extension of the realm of Kondo physics has been offered in 1988, when the idea of underbarrier tunneling in presence of Kondo center was extended on the tunneling between metallic electrodes and nanoobjects like quantum dots or small metallic grains [14,15]. Such nanoobject may serve as a Kondo center (a localized moment) provided (i) the electron spectrum is discrete due to spatial quantization, so that the level spacing $\delta\varepsilon$ exceeds the tunneling rate, (ii) Coulomb blockade prevents charge fluctuations and (iii) the electron occupation number is *odd*, so that the effective spin of the nanoobject is $1/2$. In this case the tunneling Hamiltonian may be mapped on the effective spin Hamiltonian (1), and the Kondo-like singularity arises as a zero-bias anomaly (ZBA) in tunnel transparency. This theoretical prediction was confirmed ten years later [16–18] in the experiments on planar quantum dots. Many experimental and theoretical studies then followed this experimental breakthrough ever since.

Another facet of Kondo physics in nanoobjects was unveiled, when the possibility of Kondo effect in quantum dots with *even* electron occupation number was considered in several theoretical publications [19–22]. In this case the quantum with dot a singlet ground state may become magnetically active due to external forces, and Kondo effect arises either at finite energy [19] or in external magnetic field [20–22]. Later on it was recognized that in many cases the direct mapping of the original Kondo model into such system is impossible, because the *effective* symmetry of the pertinent nanoobject is neither $SU(2)$ nor $SU(2N)$. The aim of this short review is to describe various physical situations where the underlying nanoobject possesses complex (and in some sense unusual) symmetries which are characterized by non-compact Lie groups or combinations of such groups with discrete groups of finite rotations.

Surplus symmetries

Among the sources of surplus symmetries which enrich Kondo physics of nanoobjects one may find both discrete and continuous rotations stemming from complicated geometrical configurations of complex quantum dots, as well as those induced by external fields used in practical realizations of nanodevices. In this short review we will refrain from description of great variety of these devices, which may be found in current literature (see, e.g., [23–25]). Fortunately, most of the relevant physics may be exposed in a relatively simple situation of electron tunneling through multivalley quantum dots in contact with metallic electrodes (leads).

A multivalley dot is an island with electrons confined by electrostatic potential in such a way that the spatially quantized electrons are distributed between several valleys. These valleys are coupled with each other by capacitive interaction and tunneling channels. Up to now there are several realizations of quantum dots with two and three valleys (double quantum dot, DQD, and triple quantum dot, TQD, respectively). Experimentally, the first such realizations of DQDs go back to mid 90-es [26–28]. It was pointed out that these objects can be treated as some forms of coupled artificial molecules with each dot playing the role of an artificial atom [29–32].

Compared with DQD, fabrication of TQD is a much more difficult experimental task and the first experimental realizations of these nanoobjects appeared only recently. One may mention in this connection the realization of TQD with an «open» central valley [33]. The term «open» here means that the tunneling between the side dots and the adjacent leads is limited by strong Coulomb blockade (see below), whereas the central dot freely donates and accepts electrons to and from its own reservoir, so its role in the device is only to mediate indirect exchange between the two side dots. Another successful attempt to fabricate a TQD was recorded in response to a theoretical proposal [34] to use this geometry for realization of ratchet effect in tunneling through nanoobjects. In this realization [35] the charge fluctuations were suppressed by the Coulomb blockade mechanism in all three valleys. The feasibility of filling the TQD with 1, 2 and 3 electrons by changing the gate voltages was demonstrated quite recently [36].

Theoretical studies of electronics in TQD geometry were also inspired by possible applications in the field of quantum information [37,38]. Experimental observation of molecular trimers Cr_3 on gold sublayers [39] by means of the tunnel electron spectroscopy, gave an impact to the theory of Kondo effect in TQD [40]. Later on, other properties of molecular trimers such as the two-channel Kondo effect [41,42] and the interplay between the Kondo effect and Aharonov–Bohm effect in tunnel spectroscopy [43] were considered theoretically.

Our main focus of interest is a theoretical modeling of a device consisting of a triple quantum dot, metallic

electrodes and corresponding gates. The latter regulate the electron occupation of any particular valley and of the dot as a whole. These and properties other are predetermined by the geometrical position of the valleys relative to the metallic leads (source and drain) in the device. Triple quantum dots (TQD) provide theoreticians (and experimentalists as well) with a rich variety of geometrical configurations and possess more symmetries (Fig. 1). Similarly to DQD these trimers may be oriented both in sequential (vertical) and parallel (lateral) geometries (Fig. 1,*a* and 1,*b*, respectively). The natural generalization of the T-shape geometry presented in Fig. 1,*c* is the cross geometry (Fig. 1,*c*). Besides, TQD may be organized in a form of a triangle, which may form a closed or open element in an electronic circuit (Figs. 1,*d*,*e* and 1,*f*, respectively). In the two latter cases one deals with a three-terminal tunnel device. We will call the conformations shown in Figs. 1,*e* and 1,*f* «ring» and «fork» configurations.

Let us discuss the discrete symmetry elements characteristic for the above TQD configurations. If all three valleys are equivalent, the discrete symmetry of an isolated linear TQD is that of the permutation group P_3. The contact with the leads adds one more symmetry element, the $(s-d)$-reflection, provided all three dots are coupled with the leads. We however consider the devices, where the central dot (filled black) is not coupled directly with the leads. Then the P_3 symmetry is lost. The only discrete symmetry element, namely $(s-d)$-reflection is left in a vertical geometry (Fig. 1,*a*), whereas both $(s-d)$- and $(l-r)$-reflections (which is equivalent to P_2 permutation) characterize the symmetry of lateral TQD (Fig. 1,*b*). The same is valid for the cross geometry of Fig. 1,*c*. The P_3 symmetry is inherent in the three-terminal configuration of Fig. 1,*e*. In this case it is better to use the classification of discrete rotation group C_{3v}, which is isomorphic to the permutation group P_3. One may say [43] that in the perfect triangular configuration the TQD imposes its C_{3v} symmetry on the device as a whole in close analogy with the Coqblin–Schrieffer–Cornut version [8,9] of the conventional Kondo problem. In the geometries of Fig. 1*d*,*f* the only element which is remained of the original symmetry of triangle is the $(l-r)$-symmetry like in the cross geometry. *External magnetic field* applied perpendicularly to the plane of the triangle lowers the symmetry of a device by adding one more element, that is, chirality of the electron tunneling from the source to the drain.

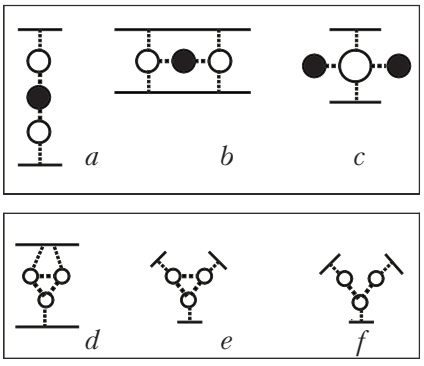

Fig. 1. Triple quantum dot in sequential (*a*), parallel (*b*), cross-shape (*c*), two-terminal triangular (*d*), three-terminal triangular (*e*) and fork (*f*) geometries.

Before considering the consequences of these symmetries for the Kondo physics, several introductory remarks about the derivation of the Kondo Hamiltonian are in order. The generally accepted approach is based on the assumption that electrons injected from the source *do not lose coherence* when propagating through the sequence of quantum dots until they leave the chain for the drain electrode. This approach is valid only provided the tunneling W between the adjacent valleys exceeds the tunneling V between the dot and the metallic leads. Working in this paradigm, one should derive the effective exchange Hamiltonian $H_{\rm ex}$ in accordance with the following procedure. The starting Hamiltonian is chosen in the same form as the original Anderson impurity Hamiltonian [6]:

$$H = H_{\rm band} + H_{\rm dot} + H_t \qquad (2)$$

where $H_{\rm dot}$ describes the properties of a chain detached from the lead *in terms of its eigenstates* $|\Lambda\rangle$:

$$H_{\rm dot} = \sum_{\Lambda} E_{\Lambda} |\Lambda\rangle\langle\Lambda| + Q(\hat{N} - \mathcal{N}). \qquad (3)$$

Here $\hat{N}$ is the operator of total electron number in the dot. The last term in (3) describes the Coulomb blockade mechanism: the total occupation of the dot $\mathcal{N}$ in neutral and charged states is fixed by the Coulomb blockade parameter Q entering the capacitive energy of a complex quantum as dot a whole. The eigenvalues E_{Λ} are found at fixed occupation $\mathcal{N}$ of DQD or TQD with all tunneling matrix elements W and interdot capacitive interactions Q' taken into account. The tunneling Hamiltonian H_t intermixes the states from adjacent charge sectors $\mathcal{N}$, $\mathcal{N} \pm 1$ due to injection of extraction of an electron from the complex dot:

$$H_t = \sum_{\Lambda\Lambda'} \sum_{b=s,d} \sum_{k\sigma} V_{bk\sigma}^{\Lambda\Lambda'} c_{bk\sigma}^{\dagger} X^{\Lambda\Lambda'} + \text{h.c.} \qquad (4)$$

where $X^{\Lambda\Lambda'} = |\Lambda\rangle\langle\Lambda'|$ are the universal Hubbard operators [44]. The tunnel parameters $V_{bk\sigma}^{\Lambda\Lambda'}$ are usually approximated by a single parameter V. In the Hamiltonian (4) these configuration changing opera-

tors describe transitions between the states belonging to different charge sectors (one of this sectors corresponds to the neutral CQD and another belong to positively or negatively charged CQD. The index b enumerates the leads ($b = s,d$ in the two-terminal configurations).

The Hamiltonian $H_{\rm band}$ has the standard form

$$H_{\rm band} = \sum_{bk\sigma} \varepsilon_k c^{\dagger}_{bk\sigma} c_{bk\sigma}. \qquad (5)$$

Comparing to the corresponding term in (1), this Hamiltonian contains one more index b. In the geometries with $(s-d)$-reflection symmetry one may rotate the frame in such a way that the band operators are classified as even and odd operators relative to this reflection

$$c_{ek\sigma} = 2^{-1/2}(c_{sk\sigma} + c_{dk\sigma}),$$
$$c_{ok\sigma} = 2^{-1/2}(c_{sk\sigma} - c_{dk\sigma}). \qquad (6)$$

In case of single and double quantum dots this rotation usually excludes the odd combination from the tunneling Hamiltonian [14]. However, it is not necessarily the case for TQD.

The cotunneling (exchange) Hamiltonian is usually obtained from (2) by means of the Schrieffer–Wolff (SW) canonical transformation [4], which excludes the states $|\Lambda\rangle$ belonging to the charge sectors $\mathcal{N} \pm 1$ from the effective Fock space. At fixed $\mathcal{N}$ we are left solely with spin degrees of freedom. In the conventional situation, the relevant symmetry is $SU(2)$ and the SW procedure results in an effective Hamiltonian (1), where exchange constant J is estimated as $J = V^2/E_C$, and E_C is expressed via addition and extraction energies, i.e. the energy costs to add or subtract an electron on/from the quantum dot:

$$E_C^{-1} = E_+^{-1} + E_-^{-1}$$
$$E^+ = \varepsilon_d + Q - \varepsilon_F, \quad E^- = \varepsilon_F - \varepsilon_d \ . \qquad (7)$$

In case of even $\mathcal{N}$ and geometries including discrete rotations, the situation is more complicated, and the SW procedure intermixes the states $|\Lambda\rangle$ belonging to different irreducible representations of the Hamiltonian (3). The corresponding terms in the effective Hamiltonian may be expressed by means of the corresponding Hubbard operators $X^{\Lambda\Lambda'}$. In many cases, combinations of these operators form closed algebras which generate non-compact groups $SO(N)$ or $SU(N)$ with $N > 2$, describing the *dynamical symmetry* of complex quantum dots. Involvement of these dynamical symmetries turns the procedure of mapping the tunnel problem onto an effective exchange problem to be more complicated than in the simpler situations which were briefly described in first Section. New features of the Kondo effect arising as a result of this procedure were described for the first time using the T-shaped DQD as an example [32]. Various manifestations of dynamical symmetries in physical problems are described in the monongraphs [45,46]. Some mathematical aspects of the dynamical symmetries as applied to the Kondo problem may be found in the recent reviews [47,48].

Kondo physics for linear TQD

From the point of view of basic symmetries there is much in common between the Kondo tunneling through DQD and TQD in linear geometry because both of them possess the permutation symmetry P_2. In case of linear TQD shown in Fig. 1,$a-c$ this the permutation of two equivalent side dots. At present, the tunneling through this simplest DQD is well understood (see [49] for a review). It turned out that the most general description of Kondo tunneling through vertical DQD may be given in terms of $SU(4)$ and $SO(4)$ symmetries of a low-energy multiplets in cases of odd and even electron occupation $\mathcal{N}$, respectively.

We discuss below the configurations where the central differs dot from two side dots in its size (and hereby by the magnitude of the Coulomb blockade parameter Q_c, but the latter dots are identical, so that the TQD retains its mirror symmetries. Both conceivable situations, namely $Q_c >> Q_s$ and $Q_c << Q_s$ will be considered (the indices c,s are used in this section to indicate the physical quantities related to the central and side dots, respectively). In the first experimental realization of TQD [33] the former option was chosen, whereas the first theoretical study [50] was devoted to to the second possibility.

In a TQD with «open» central dot and $Q_c << Q_s$, its role in formation of Kondo tunneling regime reduces to providing the channel for indirect RKKY-type mechanism of exchange between two localized spins formed in side dots. Thus, from the theoretical point of view this problem is in fact may be mapped onto that for a DQD with even electron occupation $\mathcal{N} = 2$. The Kondo effect may be described in terms of two-site Kondo Hamiltonian, where the trend to interdot spin coupling competes with the trend to individual Kondo coupling between two side dots and the electrons in the leads [51,52].

One may try to describe this problem by means of two spin operators $\mathbf{s}_l$ and $\mathbf{s}_r$ using the above mentioned analogy with the two-site Kondo problem [53]. However, such approach [54] should be used with some caution. One should take into account that in a situation, where both triplet and singlet two-electron states are involved in Kondo effect, these spins are

non-independent because the kinematical constraint is imposed on the S/T manifold by the Casimir operator $\mathcal{C} \neq \mathbf{s}_l^2 + \mathbf{s}_r^2$. In accordance with the prescriptions of the theory of dynamical symmetries [45–47], two operators

$$\mathbf{S} = \mathbf{s}_l + \mathbf{s}_r, \quad \mathbf{R} = \mathbf{s}_l - \mathbf{s}_r \tag{8}$$

should be constructed and the kinematic constraint

$$\mathcal{C} = \mathbf{S}^2 + \mathbf{R}^2 = 3 \tag{9}$$

should be imposed on them. Then the three components (S^z, S^+, S^-) of the vector $\mathbf{S}$ describe the states within the spin triplet and transitions between them, whereas the three components (R^z, R^+, R^-) of the vector $\mathbf{R}$ describe transitions between the singlet S and the states with spin projections $\mu = 1,0,-1$ of the triplet T. Six components of the vectors $\mathbf{S},\mathbf{R}$ form a closed algebra

$$\begin{aligned} [S_\alpha, S_\beta] &= ie_{\alpha\beta\gamma} S_\gamma, \\ [R_\alpha, R_\beta] &= ie_{\alpha\beta\gamma} S_\gamma, \\ [R_\alpha, S_\beta] &= ie_{\alpha\beta\gamma} R_\gamma. \end{aligned} \tag{10}$$

and form a set of generators of $SO(4)$ group. Here α,β,γ are Cartesian coordinate indices, and $e_{\alpha\beta\gamma}$ is the anti-symmetric Levi-Civita tensor. Two vector operators are orthogonal, $\mathbf{S} \cdot \mathbf{R} = 0$. Under these constraints, two vectors $\mathbf{s}_{l,r}$ are rather fictitious than real spin operators. If one tunneling channel couples this «spin rotator» with the reservoir of conduction electrons, then the dynamical group $SO(4)$ exhausts the spin degrees of freedom involved in Kondo tunneling. More detailed discussion of interconnections between two representations as well as the derivation of these operators by means of the Hubbard operators $X^{\Lambda\Lambda'}$ may be found in [32], where this scenario was realized for the first time in DQD with the T-shape geometry.

Further reduction of the problem from DQD with two sites to a single QD with two orbital is also possible.

Generic features of Kondo effect in TQD are seen in the limit $Q_c >> Q_s$ for sequential and parallel configurations of Fig. 1,*a*,*b* [50]. To demonstrate these features let us consider TQD with in lateral geometry in more details. Genesis of spin multiplets may be understood from a general set-up illustrated by Fig. 2. In case of $\mathcal{N} = 3$ three electrons are distributed over three dots in such a way that the state with doubly occupied central is dot suppressed by strong Coulomb blockade Q_c. In accordance with the Young tableaux for a system with $(l-r)$-permutation symmetry, the spin multiplet consists of two doublets with $S = 1/2$ having even and odd symmetry relative to this permutation and one quartet $S = 3/2$ with full orbital symmetry. In case of $\mathcal{N} = 4$ the spin manifold consists of two spin singlets $S_{e,o}$ and two triplets $T_{e,o}$, both even and

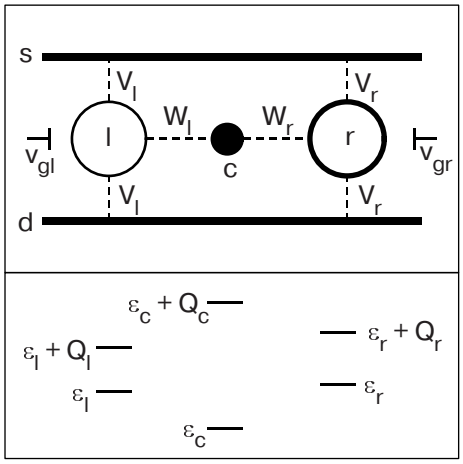

Fig. 2. TQD in parallel geometry and energy levels of each dot $\varepsilon_a - ev_{ga}$ at $W_a = 0$.

odd relative to $(l-r)$-permutation. Varying the gate voltages v_{gl}, v_{gr} and playing with tunnel parameters $V_{l,r}$ and $W_{l,r}$, one may break $(l-r)$-symmetry (Fig. 2) and change the singlet-triplet splitting, so that the spin states are classified as $S_{l,r}$ and $T_{l,r}$. The relative positions of energy levels in spin multiplets evolve as a function of model parameters and various types of level crossings occur (see [50] for detailed calculations). Similar situation arises for vertical configuration of Fig. 1,*a*.

In accordance with general theory of dynamical symmetries [47], quasi degeneracy of low-lying states in spin multiplets within the Kondo energy scale $\sim T_K$ generates special symmetries of TQD. The simplest example of dynamical symmetry is a S/T multiplet, where the two vectors $\mathbf{R}_1, \mathbf{R}_2$ generate the group $SO(4)$ with the kinematic constraint (9). If the multiplet of low-lying states within a scale T_K consists of two singlets and one triplet, the relevant dynamical symmetry is $SO(5)$. If this multiplet is formed by two triplets and one singlet, the corresponding symmetry is $SO(7)$, etc. 10 generators, which form the o_5 algebra for the group $SO(5)$ are the spin vector $\mathbf{S}$ with three components describing transitions within the triplet $S = 1$, two three-component vectors $\mathbf{R}_1, \mathbf{R}_2$, which describe transitions between two singlets and triplet, and the scalar A describing transitions between two singlets. The algebra o_7 contains 21 generator for the group $SO(7)$. These are two spin vectors $\mathbf{S}_1, \mathbf{S}_2$ corresponding to the irreducible representations for two triplets, plus four vectors $\mathbf{R}_{1-4}$ and three scalars A_{1-3} corresponding to various transitions between singlet and two triplets. The methods of constructing these generators my means of Hubbard operators and/or fermionization procedure are described in de-

tails in the reviews [47,48] and in the thesis [55]. Casimir constraint for $SO(n)$ group has the form

$$\sum_i \mathbf{S}_i^2 + \sum_i \mathbf{R}_i^2 + \sum_i A_i^2 = n - 1 . \qquad (11)$$

Dynamical symmetry is activated by the cotunneling processes between the TQD and the electron continuum in metallic leads. Cotunneling transitions induce transitions between different levels in the spin multiplet. These transitions are spin flips in conventional theory of Kondo effect, but in the systems with complex symmetry non-diagonal transitions between the states belonging to different irreducible representations of spin-multiplet described by the operators $\mathbf{R}_i$ also arise. As a result the SW procedure [4] generates the generalized exchange Hamiltonian

$$H_{\rm ex} = 2\sum_{ij} J_{ij}\mathbf{S}_i \cdot \mathbf{s}_j + 2\sum_i \tilde{J}_i \mathbf{R}_i \cdot \mathbf{s}_j . \qquad (12)$$

The spin operators for conduction electrons $\mathbf{s}_j$ are determined in a usual way [see Eq. (1)], but the index j stands for even and odd combinations (6) of lead electron wave functions. Unlike the case of single quantum dot [14], the odd mode is not eliminated from the tunneling Hamiltonian [56]. The number of scaling equations for the system (12) depends on the spin symmetry of TQD, and the latter may be changed by varying the parameters of the basic Hamiltonian (2).

The complex phase diagram characterizing Kondo effect in TQD may be constructed by means of the perturbative (high-temperature) renormalization group (RG) approach. This approach is based on the study of flow diagrams describing the evolution of effective coupling parameters $J_a(\eta)$ due to reduction of the effective energy scale D of conduction electron kinetic energy [57] (label a enumerates the vertices in the exchange Hamiltonian, $\eta = \ln D$ is the scaling variable). The general form of the system of scaling equations is

$$\frac{dj_a}{d\eta} = -\sum_b c_{ab} j_a j_b . \qquad (13)$$

Here $j_a = \rho J_a$ are dimensionless coupling constants and c_{ab} are numerical coefficients. These equations should be solved under the boundary conditions $j(D_0) = \rho J_{a0}$, where D_0 and J_{a0} are the initial conduction bandwidth and the bare exchange integrals entering the Hamiltonian $H_{\rm ex}$.

As a result, a unique opportunity arises to change the value of index n characterizing the symmetry $SO(n)$ of TQD by varying the gate voltages and other experimentally controllable parameters of a device. The phase diagram of vertical TQD with $\mathcal{N} = 4$ calculated in [50] is shown in Fig. 3.

This diagram shows great variety of phases with different symmetries from the most symmetric one $P_2 \otimes SO(4) \otimes SO(4)$ to conventional $SO(3)$ phase where the ground state of TQD is spin triplet, or non-Kondo singlet ground state (shaded areas). Each phase is characterized by its own Kondo temperature, which deviates from the the standard equation for T_K given by equation $T_K = D\exp(-1/2\rho J)$, where D is the characteristic energy scale for the band electrons in the leads and ρ is the density of states at the Fermi level ε_F. ZBA in tunnel transparency at $T > T_K$ follows the scaling law

$$G_{\max}(T)/G_0 \sim \ln^{-2}(T/T_K) \qquad (14)$$

where $G_0 = 2e^2/h$ is the limiting value of tunnel conductance in a Kondo regime (unitarity limit, where the sum of all phase shifts on the Fermi levels $\delta_{i\sigma}$ equals $\pi/2$). The limiting value quantify the tunnel conductance at $T - 0$. This means that the ZBA in conductance should follow the change of the Kondo temperature, so that each crossover from one symmetry to another is accompanied by the abrupt change of conductance at given temperature. The physical nature of variation of T_K in the process of crossover from one dynamical symmetry to another will be explained in the next section where the TQD in «cross» and «fork» geometries illustrated by Fig. 1*c*,*f* will be considered in more details.

At $\mathcal{N} = 3$ we meet a somewhat unexpected situation where Kondo tunneling in a quantum dot with *odd* occupation demonstrates the exchange Hamiltonian of a quantum dot with *even* occupation. The reason for this scenario is the specific structure of the wave function of TQD with $\mathcal{N} = 3$. The corresponding wave functions are vector sums of states composed of a «passive» electron sitting in the central and dot singlet/triplet (S/T) two-electron states in the l,r dots. Then using certain Young tableaux [50], one concludes that the spin dynamics of such TQD is repre-

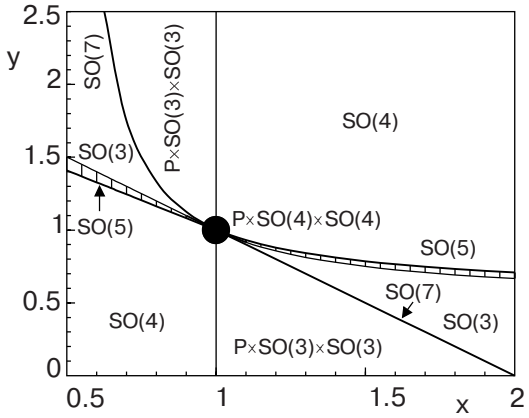

Fig. 3. Dynamic symmetries in TQD: phase diagram in coordinates $x = (V_l/V_r)^2$, $y = (\varepsilon_l - \varepsilon_c)/(\varepsilon_r - \varepsilon_c)$.

sented by the spin 1 operator **S** corresponding to the $l-r$ triplet, the corresponding operator **R** and the spin 1/2 operator $\mathbf{s}_c$ of a passive electron in the central well. The latter does not enter the effective Hamiltonian $H_{\rm ex}$ but influences the kinematic constraint via the Casimir operator

$$C = \mathbf{S}^2 + \mathbf{M}^2 + \mathbf{s}_c^2 = \frac{15}{4}. \qquad (15)$$

The dynamical symmetry is therefore $SO(4) \otimes SU(2)$, and only the $SO(4)$ subgroup is involved in Kondo tunneling. Similar situation, although for different reasons is realized in fork and cross geometries (see below).

Remarkable symmetry reduction occurs in external magnetic field [50]. First example of such reduction was found in a situation where the exchange splitting of S/T multiplet (symmetry group $SO(4)$) is compensated by the Zeeman splitting [20], so that the up spin projection $|T1\rangle$ of triplet forms a pseudospin with singlet $|S\rangle$ and the symmetry reduction $SO(4) \to SU(2)$ takes place. In case of TQD with $SO(5)$ symmetry, due to the same compensation the system may be left in a subspace $\{T1_l, S_l, S_r\}$. The symmetry reduction in this case is $SO(5) \to SU(3)$, and the Anderson Hamiltonian is mapped on a very specific *anisotropic* Kondo Hamiltonian involving only operators $\mathbf{R}_i$,

$$H_{\rm ex} = \sum_{ij} \sum_{\mu\nu} J_{ij}^{\mu\nu} R_i^{\mu} s_j^{\nu}, \qquad (16)$$

where μ, ν are cartesian components of scalar product. Here the Kondo effect is described exclusively in terms of dynamical symmetry.

Another non-standard manifestation of Kondo mapping for linear TQD is the possibility of two-channel Kondo effect in vertical geometry of Fig. 1,*a* with $Q_c >> Q_s$ at $\mathcal{N} = 3$ with preserved $(s-d)$-mirror symmetry [56]. The strong Coulomb blockade in central dot prevents direct $(s-d)$-tunneling. The cotunneling is possible only because the wave functions of electrons centered on the side dots have small tails on the central dot. It is crucially important that the standard rotation (6) does not eliminate the odd channel from the tunneling Hamiltonian in TQD. In the situation, where the ground state of TQD is the spin doublet with even parity $|D_e\rangle$, the SW transformation for the original Anderson Hamiltonian results in anisotropic two-channel exchange Hamiltonian,

$$H_{\rm ex} = J_s \mathbf{S} \cdot \mathbf{s}_s + J_d \mathbf{S} \cdot \mathbf{s}_d + J_{sd} \mathbf{S} \cdot (\mathbf{s}_{sd} + \mathbf{s}_{ds}). \qquad (17)$$

In accordance with the theory of two-channel Kondo effect [12], the presence of nondiagonal vertex J_{sd} makes the 2-channel fixed point unattainable, but due to strong Coulomb blockade in central dot $J_{sd} \simeq V^2 W^2 / Q_c \varepsilon_d^2$ is extremely small, so that one may approach the fixed point close enough, and the predecessor of 2-channel regime may be observed experimentally as a dip in conductance G as a function of the difference of gate voltages $v_{gs} - v_{gd}$ applied to the side dots (this difference controls the degree of channel anisotropy).

TQD in cross and fork geometry

We have seen above that one may meet the situation, where the linear TQD with odd occupation and half-integer spin demonstrates the Kondo physics characteristic for even occupation with integer spin due to the fact that one of the electrons in the does dot not participate in tunneling. Here we will discuss two more mechanisms of such «disguise» [58].

One of these mechanisms is realized *in cross geometry* at occupation $\mathcal{N} = 3$ under condition $Q_s >> Q_d$ for Coulomb blockade parameters. In this case two side electrons are passive: the tunneling between source and drain occurs through the central dot. However, these passive electrons influence Kondo mapping because they are responsible for the *parity* of the 3-electron wave function relative to the $(l-r)$-reflection. Diagonalization of the low-energy spin states shows that it consists of three spin doublets and one spin quartet, and the lowest state in this manifold is the doublet D_u, which is odd relative to the mirror reflection (see [58] for details). Although the wave functions of two passive electrons do not enter explicitly in the indirect exchange integral arising due to SW transformation, this integral changes its sign due to odd parity of the state D_u. Thus, in contrast to the standard paradigm of Kondo mapping, the effective exchange Hamiltonian corresponds to ferromagnetic coupling, which is irrelevant to Kondo effect, and the Kondo-type ZBA does not arise in this case in spite of the fact that the net spin of quantum dot is 1/2.

However, this is not the end of the story. The excited states in the spin multiplet which are Kondo active, influence the tunnel transparency and conductance at finite temperature and finite energies of incident electron due to non-trivial dynamical symmetry of TQD described above. The states involved in the Kondo effect are the even spin doublet D_g and the quartet Q, so that the overall dynamical symmetry of TQD in cross geometry is $SU(2) \otimes SU(2) \otimes SU(2)$. Similar situation is known as a «two-stage» Kondo effect in DQD with $\mathcal{N} = 2$, on the singlet side of S/T crossover (see [49] and references therein). At high enough energy or temperature exceeding the width of the spin multiplet all spin states are involved in Kondo screening. With decreasing energy in the course of the RG renormalization the high-energy lev-

els are quenched and only the lowest spin state is responsible for the tunneling at $T \to 0$.

In our case there are three stages of Kondo screening, where the states Q and D_g are quenched one after another with decreasing energy or temperature and the Kondo screening eventually stops at zero T. Besides, the level crossing may occur because of the many-body logarithmic renormalization [59,60], which is determined by the renormalization group invariants E^*_Λ, namely

$$E^*_\Lambda = E_\Lambda(D) - \pi^{-1}\Gamma_\Lambda \ln(\pi D/\Gamma_\Lambda). \qquad (18)$$

The level crossing occurs because the hierarchy of tunneling rates $\Gamma_Q > \Gamma_{Dg} > \Gamma_{Du}$ takes place. This crossover shown in Fig. 4 is controlled by the parameters of TQD. Here the scaling variable is chosen in the form $\eta = \ln(\pi D/\Gamma_Q)$. The value of $\overline{D}$ is determined from the crossover condition $\overline{D}_\Lambda \approx E_\Lambda(\overline{D}_\Lambda)$, where the renormalization (18) changes for the SW regime with fixed charge, $\overline{D}_0$ is the initial value of scaling variable.

Three points $(\ln \overline{d}_u, \ln \overline{d}_Q, \ln \overline{d}_{\rm cr},)$ on the abscissa axis correspond to three values of the control parameters where the crossover to the SW regime occurs for the ground states E_{D_u}, E_Q and the completely degenerate ground state, respectively. By means of appropriate variation of the control parameters, the system may be transformed from a non-Kondo regime with the ground state E_{Du} to the underscreened Kondo regime with the ground state E_Q and spin $S = 3/2$. In accordance with the general theory of Kondo mapping, T_K is maximum in the point of maximum degeneracy. Evolution of T_K is shown in Fig. 5. Unlike the case of singlet/triplet crossover in DQD with $\mathcal{N} = 2$, here one deals with the crossover from the non-Kondo spin doublet D_u to the Kondo spin quartet Q via the highly degenerate region of $SU(2) \otimes SU(2) \otimes SU(2)$ symmetry.

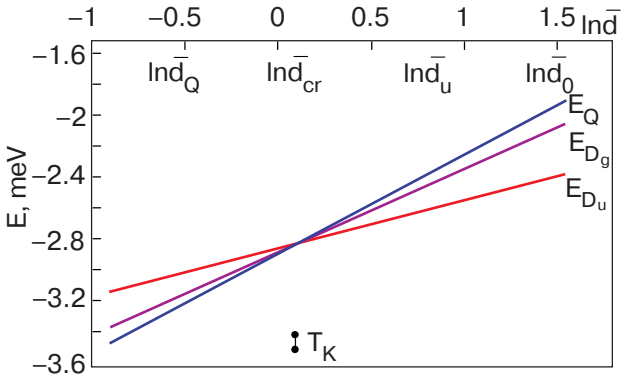

Fig. 4. Flow diagram for the levels E_Λ determined by the scaling invariant (18). $\Lambda = D_u, D_g, Q$, $\overline{d} = \pi\overline{D}/\Gamma_Q$. Energy is measured in meV units (see text for further explanations).

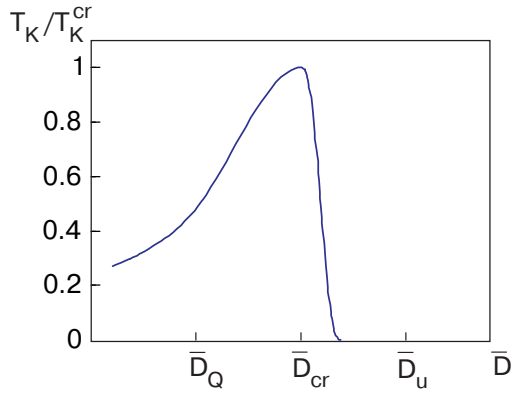

Fig. 5. Evolution of T_K in cross geometry as a function of a control parameter $\overline{D}$.

Let us now turn to the *fork geometry* shown in Fig. 1,*f*. In this geometry non-trivial Kondo physics arises already in the simplest case of odd occupation $\mathcal{N} = 1$ in a situation with the $(l-r)$-mirror symmetry. The fork may be considered as a «quantum pendulum» [38,61]. Three one-electron eigenvalues are

$$E_{D_{b,a}} = \varepsilon_s \mp 2W^2/\Delta, \quad E_{D_n} = \varepsilon_c, \qquad (19)$$

($\Delta = \max\{|\varepsilon_s - \varepsilon_c|, |Q_c - Q_s|\}$). The eigen modes are classified as a non-bonding spin doublet D_n (odd combination of the wave functions centered in the sites 1,2) and bonding/antibonding pair $D_{b,a}$ of corresponding even conbination with the state centered in the cite 3 (see [58] for details). The latter pair is the analog of resonant valence bonds (RVB) known in «natural» molecules. To describe this pendulum one should introduce the pseudospin vector $\mathcal{T}$

$$\mathcal{T}^+ = \sum_\sigma |Db\sigma\rangle\langle Dn\sigma|, \quad \mathcal{T}^- = [\mathcal{T}^+]^\dagger,$$

$$\mathcal{T}^z = \frac{1}{2}\sum_\sigma (|Db\sigma\rangle\langle Db\sigma| - |Dn\sigma\rangle\langle Dn\sigma|). \qquad (20)$$

together with similar vector $\mathbf{t}$ for conduction electrons

$$t^+ = \sum_{k\sigma} c^\dagger_{ek\sigma} c_{ok\sigma}, \quad t^- = [\tau^+]^\dagger,$$

$$t_z = \frac{1}{2}\sum_{k\sigma} (c^\dagger_{ek\sigma} c_{ek\sigma} - c^\dagger_{ok\sigma} c_{ok\sigma}). \qquad (21)$$

Here the states labeled as e,o are the even and odd combinations for the electrons in the leads 1,2 similar to those in Eq. (6). In this situation the effective exchange Hamiltonian has the form

$$H_{SW} = \sum_{\kappa\lambda\mu\rho} J_{\kappa\lambda\mu\rho} \mathbf{S}_{\kappa\lambda} \cdot \mathbf{s}_{\mu\rho} + J_p \mathbf{T} \cdot \mathbf{t} \qquad (22)$$

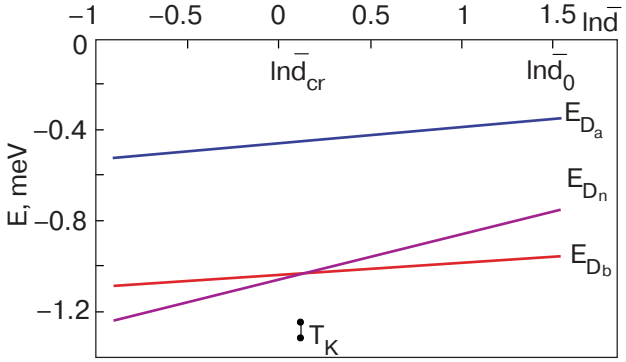

Fig. 6. Flow diagram for the levels E_Λ of the TQD in fork geometry.

with $\kappa,\lambda = b,n$; $\mu,\rho = e,o$. The five vector operators $\mathbf{S}_{\Lambda\Lambda'}$ and $\mathbf{T}$ constitute the 15 generators of the $SU(4)$ group.

Like in the cross geometry, the level crossing effect as a function of control parameter takes place (Fig. 6). Now T_K is nonzero on both sides of the crossover and its evolution is described by the bell-like curve shown in Fig. 7. Maximum $T_K^{\rm cr}$ on this curve correspond to the degeneracy point on the flow diagram of Fig. 6. However the tunnel conductance is drastically influenced by the pendulum structure of the electron wave function. In the three-terminal fork geometry, one should consider separately the situations, where the bias voltage is applied between the leads 1 and 2 and between the leads 1 and 3. We define the corresponding components of tunnel conductance as G_{22} and G_{33}, respectively. The Kondo anomaly in G_{22} is predetermined by the RVB pair, and the ZBA roughly follows the evolution of T_K through the crossover. More peculiar behavior is expected in 1–3 channel because the non-bonding state $D_{n\sigma} = 2^{-1/2}(d^\dagger_{1\sigma} - d^\dagger_{2\sigma})$ is detached from the lead 3. As a result the Kondo contribution to G_{33} manifests itself as a finite bias anomaly (FBA) in a situation where the ground state of TQD is E_{D_n}. Tunnel conductance as a function of bias voltage in both channels is illustrated in Fig. 8. The dip in the curve *b* on the right panel reminds similar dip in the tunnel conductance of DQD with $\mathcal{N} = 2$ on the singlet side of S/T crossover [62,63].

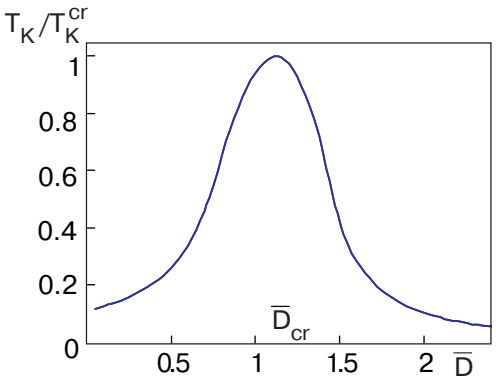

Fig. 7. Evolution of T_K in fork geometry.

Thus, we see that some manifestations of the Kondo effect in TQD with odd occupation may mimic those for DQD with even occupation due to specific influence of the mirror reflection on the structure of the electron wave functions in trimers.

Kondo physics in triangular quantum dots

It was noticed in [40] that the basic symmetry of equilateral triangular triple quantum dot (TTQD, Fig. 1,*e*) with odd occupation is $SU(4)$ due to the interplay between the spin and orbital degrees of freedom, similar to that in two-orbital DQD. Special attention was paid to the case $\mathcal{N} = 3$ which models

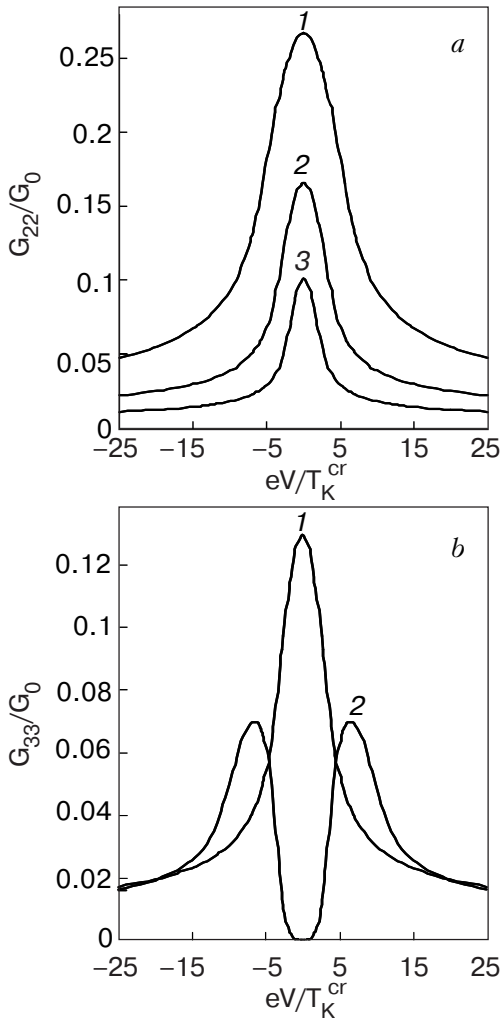

Fig. 8. Tunnel conductance in the channel 2–1 for $\overline{D} = \overline{D}_{\rm cr}$ (*1*), $\overline{D} > \overline{D}_{\rm cr}$ (*2*) and $\overline{D} < \overline{D}_{\rm cr}$ (*3*) (*a*). Tunnel conductance in the channel 3–1 for $\overline{D} > \overline{D}_{\rm cr}$ (*1*) and $\overline{D} < \overline{D}_{\rm cr}$ (*2*) (*b*).

triangular Co trimer [42,64]. In this charge sector the effective spin Hamiltonian contains not only exchange interaction between the spins in the dots and adjacent leads, but also the two-site Heisenberg exchange between spins in the neighboring dots. Magnetic frustrations in triangular geometry affect the spin state and therefore influences the Kondo-type ZBA in tunneling spectra. These spectra were calculated by the numerical RG and quantum MonteCarlo methods. Besides, it was found [42] that in case of complete channel isotropy the non-Fermi-liquid regime arises from the interplay of magnetic frustrations and Kondo physics.

Another phenomenon, which interplays with the Kondo physics is the Aharonov–Bohm oscillation of tunnel transparency in magnetic field directed perpendicularly to the plane of triangle. This effect may be seen already for the TTQD with $\mathcal{N} = 1$, where there is no room for exchange interaction between spins localized in neighboring sites and concomitant magnetic frustrations. The starting point for solving the problem of interplay between Kondo and Aharonov–Bohm phenomena [43,65] is the Anderson Hamiltonian (2) rather than the effective exchange Hamiltonian.

In accordance with the general scheme discussed above, one should start with the diagonalization of the Hamiltonian of 3-site ring. The point symmetry of this equilateral triangle is C_{3v}. This group describes the «orbital» degrees of freedom, whereas the continuous spin symmetry is usual $SU(2)$ symmetry of spin $1/2$. According to the irreducible representations of C_{3v} group, the spectrum of TTQD consists of three states $\Lambda = DA, DE_{\pm}$. Here as usual D stands for spin doublet, A is the fully symmetric orbital singlet and $E_{\pm}$ are two components of orbital doublet. The energies of these states in out-of-plane magnetic field B are

$$E_{D\Gamma}(p) = \varepsilon - 2W\cos\left(p - \frac{\Phi}{3}\right). \qquad (23)$$

such that for negative W and for $B = 0$, $p = 0, 2\pi/3, 4\pi/3$ correspond respectively to $\Lambda = A, E_{\pm}$ with the ground state DA, so that the orbital degrees of freedom are quenched at low temperature and the SW mapping procedure ends with conventional Kondo Hamiltonian (1). However, using the magnetic field as a control parameter, one may initiate level crossing by varying the magnetic flux Φ through TTQD. This level crossing is shown on the upper panel of Fig. 9. In each crossing points and its nearest vicinity the dynamical symmetry of TTQD is $SU(4)$, so that the symmetry crossovers $SU(2)$ occur at $\Phi = (n + \frac{1}{2})\Phi_0$, where Φ_0 is the quantum of magnetic flux. Each crossover is accompanied by the change of T_K from $\exp(-1/2J)$ to $\exp(-1/4J)$ and back. The

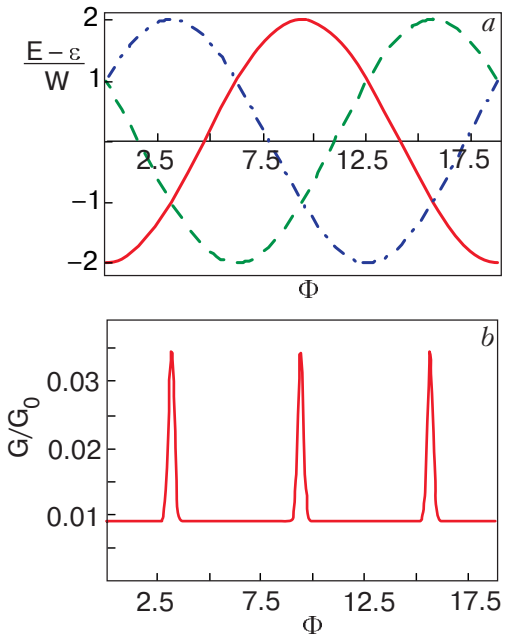

Fig. 9. Evolution of the energy levels E_A (solid line) and $E_{\pm}$ (dashed and dash-dotted line, resp.) (*a*). Corresponding evolution of conductance ($G_0 = \pi e^2/\hbar$) (*b*).

ZBA peak in the two-terminal tunnel conductance changes accordingly (Fig. 9,*b*).

Although formally there are three tunneling channels, the non-Fermi liquid Kondo regime cannot arise, because the non-diagonal components J_{ij} appear in the exchange Hamiltonian (12). Further diagonalization should be done by means of rotating frameworks for Bloch electrons. This diagonalization introduces irremovable channel anisotropy, so that the 2-channel non-Fermi-liquid fixed point cannot be achieved unlike the case considered in [42], where the channel isotropy was postulated from the very beginning.

In order to realize the Aharonov–Bohm interference, one should use the two-terminal geometry shown in Fig. 1,*d*. In this case there are two paths (1–3) and (2–3) for single electron tunnelling between source and drain. Interference of two waves in the drain results in famous Aharonov–Bohm oscillations. The field B affects the lead-hopping dot phases. In the chosen gauge, the hopping integrals are modified as, $W \to W\exp(i\Phi_1/3)$ $V_{1,2} \to V_s\exp[\pm i(\Phi_1/6 + \Phi_2/2)]$ where $\Phi_{1,2}$ are magnetic fluxes through the upper and lower loop of the device. As a result the exchange Hamiltonian reads

$$H = J_s\mathbf{S}\cdot\mathbf{s}_s + J_d\mathbf{S}\cdot\mathbf{s}_d + J_{sd}\mathbf{S}\cdot(\mathbf{s}_{sd} + \mathbf{s}_{ds}) + K\mathbf{T}\cdot\mathbf{t} \qquad (24)$$

(the latter term becomes actual when the magnetic field induces level crossing in accordance with Fig. 9). Magnetic flux enters the coupling constants J_s, J_d, J_{sd}, K via SW transformation. As a result the

constant $J_{sd}(\Phi_1,\Phi_2)$ turns into zero at some values of magnetic flux, so that the Aharonov–Bohm interference completely blocks Kondo transparency. Thus TTQD serves simultaneously as a Kondo «pass valve» and as an Aharonov–Bohm interferometer. It should be stressed that both the continuous spin degrees of freedom and discrete «rotations» of triangle are involved in these two phenomena in TTQD.

Concluding remarks

Among many aspects of Kondo tunneling through complex quantum dots we have chosen for this review only the symmetry related properties predetermined by the structure of the low-lying states in the spin multiplet characterizing the fixed charge sector of complex quantum dot. New features, which are introduced by the dynamical symmetries in the Kondo physics are the multistage process of Kondo screening, symmetry crossovers driven by experimentally tunable control parameters, interplay between continuous spin rotation symmetry and discrete point symmetry of nanodevices. The main tool of experimental monitoring of variable symmetries is study of temperature and magnetic filed dependence of zero- and finite-bias anomalies in tunnel conductance.

Among other novel facets of Kondo effect in nanostructures one should mention non-equilibrium Kondo effect at finite bias and under light illumination, where both quantum dots and leads are far enough from thermodynamic balance. Under this conditions such phenomena as spin relaxation, dephasing and decoherence influence the tunnel transport in Kondo regime. Real atoms and molecules also may be included in electric circuit by means of advanced experimental techniques (scanning tunnel spectroscopy, break-junction method etc). In this case phonon- and photon assisted processes should be taken into account, which result in interplay of Kondo resonance tunneling with various «polaronic» and «excitonic» effects.

1. J. Kondo, *Progr. Theor. Phys*. **32**, 37 (1964).
2. J. Appelbaum, *Phys. Rev. Lett.* **17**, 91 (1966).
3. P.W. Anderson, *Phys. Rev. Lett*. **17**, 95 (1966).
4. J.R. Schrieffer and P.A. Wolff, *Phys. Rev.* **149**, 491 (1966).
5. J. Friedel, *Can. J. Phys*. **34**, 1190 (1956).
6. P.W. Anderson, *Phys. Rev.* **124**, 41 (1961).
7. K.S. Dy, *Phys. Status Solidi* **B81**, K111 (1977).
8. B. Coqblin and J.R. Schrieffer, *Phys. Rev*. **185**, 847 (1969).
9. B. Cornut and B. Coqblin, *Phys. Rev.* **B5**, 4541 (1972).
10. I. Affleck and J. Marston, *Phys. Rev. Lett*. **37**, 3774 (1988).
11. N. Read and S. Sachdev, *Nucl. Phys*. **B316**, 609 (1989).
12. P. Nozieres and A. Blandin, *J. Phys. (Paris)* **41**, 193 (1980).
13. P. Nozieres, *J. Low Temp. Phys*. **17**, 31 (1974).
14. L.I. Glazman and M.E. Raikh, *JETP Lett.* **47**, 452 (1988).
15. T.K. Ng and P.A. Lee, *Phys. Rev. Lett*. **61**, 1768 (1988).
16. D. Goldhaber-Gordon, H. Shtrikman, D. Mahalu, D. Abusch-Magder, U.Meirav, and M.A. Kastner, *Nature* **391**, 156 (1998).
17. S.M. Cronenwett, T.H. Oosterkamp, and L.P. Kouwenhoven, *Science* **281**, 540 (1998).
18. F. Simmel, R.H. Blick, J.P. Kotthaus, W. Wegscheider, and M. Bichler, *Phys. Rev. Lett.* **83**, 804 (1999).
19. K. Kikoin and Y. Avishai, *Phys. Rev.* **B62** 4647 (2000).
20. M. Pustilnik, Y. Avishai, and K. Kikoin, *Phys. Rev. Lett*. **84**, 1756 (2000).
21. D. Giuliano and A. Tagliacozzo, *Phys. Rev. Lett*. **84**, 4677 (2000).
22. M. Eto and Yu. Nazarov, *Phys. Rev. Lett.* **85**, 1306 (2000).
23. *Single Charge Tunneling*, H. Grabert and M.H. Devoret (eds.), Plenum, New York (1992).
24. *Mesoscopic Electron Transport*, L.L. Son, L.P. Kouwenhoven, and G. Schön (eds.), Kluwer, Dordrecht (1997).
25. W.G. van der Wiel, S. De Franceschi, J.M. Enselman, T. Fujisawa, S. Tarucha, and L.P. Kouwenhoven, *Rev. Mod. Phys.* **75**, 1 (2003).
26. F. Hofmann, T. Heinzel, D.A. Wharam, J.P. Kotthaus, G. Böhm, W. Klein, G Tränkle, and G. Weimann, *Phys. Rev.* **B51**, 13872 (1995).
27. L.W. Molenkamp, K. Flensberg, and M. Kemerlink, *Phys. Rev. Lett*. **75**, 4282 (1995).
28. C. Livermore, C.H. Crouch, R.M. Westervelt et al., *Science* **274**, 1382 (1996).
29. J.J. Palacios and P. Hawrilak, *Phys. Rev*. **B51**, 1769 (1995).
30. D. Loss and D.P. DiVincenzo, *Phys. Rev*. **A57**, 120 (1998).
31. B. Partoens and F.M. Peeters, *Phys. Rev. Lett.* **84**, 4433 (2000).
32. K. Kikoin and Y. Avishai, *Phys. Rev. Lett*. **86**, 2090 (2001); *Phys. Rev*. **B65**, 115329 (2002).
33. N.J. Craig, J.M. Taylor, E.A. Lester, C.M. Marcus, M.P. Hanson, and A.C. Gossard, *Science* **304**, 565 (2004).
34. M. Stopa, *Phys. Rev, Lett*. **88**, 146802 (2002).
35. A. Vidan, R.M. Westervelt, M. Stopa, M. Hanson, and A.C. Gossard, *Appl. Phys. Lett*. **85**, 3602 (2004).
36. L. Gaudreau, S. Studenikin, A. Sachrajda, P. Zavadzki, A. Kam, J. Lapointe, M. Korkusinski, and P. Hawrilyak, *arXiv:cond-mat/06015967*.
37. T. Tanamoto, *Phys. Rev*. **A61**, 022305 (2000).

38. D.S. Saraga and D. Loss, *Phys. Rev. Lett*. **90**, 166803 (2003).
39. T. Jamneala V. Madhavan, and M.F. Crommie, *Phys. Rev. Lett*. **87**, 256804 (2001).
40. G. Zaránd, A. Brataas, and D. Goldhaber-Gordon, *Solid State Commun*. **126**, 463 (2003).
41. B. Lazarovits, P. Simon, G. Zaránd, and L. Szunyogh, *Phys. Rev. Lett*. **95**, 077202 (2005).
42. K. Ingersent, A.W. Ludwig, and J. Affleck, *Phys. Rev. Lett*. **95**, 257204 (2005).
43. T. Kuzmenko, K. Kikoin, and Y. Avishai, *Phys. Rev. Lett.* **96**, 046601 (2006).
44. J. Hubbard, *Proc. Roy. Soc*. **A285**, 542 (1965).
45. M.J. Englefield, *Group Theory and the Coulomb Problem*, Wiley, New York (1972).
46. I.A. Malkin and V.I. Man'ko, *Dynamical Symmetries and Coherent States of Quantum Systems*, Fizmatgiz, Moscow (1979).
47. K. Kikoin, Y. Avishai, and M.N. Kiselev, in: *Nanophysics, Nanoclusters, Nanodevices*, Nova Publishers, New York (2006).
48. M.N. Kiselev, *Int. J. Mod. Phys*. **B20**, 381 (2006).
49. M. Eto, *J. Phys. Soc. Jpn*. **74**, 95 (2005).
50. T. Kuzmenko, K. Kikoin, amd Y. Avishai, *Phys. Rev. Lett*. **89**, 156602 (2002); *Phys. Rev*. **B69**, 195109 (2004).
51. P. Simon, R. Lopez, and Y. Oreg, *Phys. Rev. Lett*. **94**, 086602 (2005).
52. M.G. Vavilov and L.I. Glazman, *Phys. Rev. Lett*. **94**, 086805 (2005).
53. B.A. Jones and C. Varma, *Phys. Rev.* **B40**, 324 (1989).
54. M. Pustilnik and L.I. Glazman, *Phys. Rev. Lett*. **85**, 2993 (2000); *Phys. Rev*. **B64**, 045328 (2001).
55. T. Kuzmenko, *Kondo Effect in Artificial and Real Molecules*, *Ph. D Thesis*, Ben-Gurion University, Beer-Sheva (2005); *arXiv:cond-mat/0509480*
56. T. Kuzmenko, K. Kikoin, and Y. Avishai, *Europhys. Lett*. **64**, 218 (2003).
57. P.W. Anderson, *J. Phys.* **C3**, 2436 (1980).
58. T. Kuzmenko, K. Kikoin, and Y. Avishai, *Phys. Rev*. **B73**, 235310 (2006).
59. A.F. Barabanov, K.A. Kikoin, and L.A. Maksimov, *Teor. Mat. Fiz*. **20**, 364 (1974).
60. F.D.M. Haldane, *Phys. Rev. Lett*. **40**, 416 (1978).
61. K. Le Hur, P. Recher, E. Dupont, and D. Loss, *Phys. Rev. Lett.* **96**, 106803 (2006).
62. W. Hofstatter and H. Schoeller, *Phys. Rev. Lett*. **88**, 016803 (2002).
63. W.G. van der Wiel, S. de Francheschi, T. Fujisawa, J.M. Elzerman, S. Tarucha, and L.P. Kouwenhoven, *Science* **289**, 2105 (2000).
64. V.V. Savkin, A.N. Rubtsov, M.I. Katsnelson, and A.I. Lichtenstein, *Phys. Rev. Lett.* **94**, 026402 (2005).
65. T. Kuzmenko, K. Kikoin, and Y. Avishai, *Physica* **E29**, 334 (2005).